

Field evaporation of gold in single- and double-electrode systems

N. M. Miskovsky* and Tien T. Tsong

Institute of Physics, Academia Sinica, Nankang, Taipei, Taiwan 11529, Republic of China

(Received 2 March 1992)

Field evaporation of gold as positive and negative ions in single- and double-electrode systems is investigated with the charge-exchange model using atomic potentials from an embedded-atom method and a method discussed by H. Gollisch [Surf. Sci. **166**, 87 (1986); **175**, 249 (1986)]. For the single-electrode geometry of the field-ion microscope, Au^+ should be the observable ion species. In the double-electrode geometry of the scanning tunneling microscope, Au^{2-} should be the favored ion species since it requires the lowest evaporation field.

Field evaporation, desorption of surface atoms in the form of ions by an applied electric field, is a basic physical process in field-ion microscopy (FIM).¹ It is also one of a few atomic processes now known to be useful for atomic manipulation with the scanning tunneling microscope (STM).^{2,3} In the FIM, atoms are removed from the tip surface by applying a positive electric field of the order of a few volts per angstrom. The removal of atoms can be directly observed in the FIM image and the evaporated ion species can be identified by mass spectrometry. In atomic manipulation with the STM, positive or negative voltage pulses of a few volts are applied either to the tip or to the sample. A transfer of atoms between the probing tip and the sample surface can be directly observed in the STM image, but the ion species cannot yet be experimentally identified. The field needed for field evaporation in the STM appears to be substantially lower by at least a factor than that in the FIM. For example, field evaporation of gold in the FIM requires a field of about 3.5 V/Å whereas in the STM, the field required appears to be less than 1 V/Å.²

In the FIM, field evaporation of negative ions has not yet been observed, because in a negative field, field emission can occur. At the field expected for field evaporation to occur, the field electron current will be large enough to melt the slender tips used in the FIM. Such a difficulty is greatly alleviated in the STM as has been explained earlier in a preliminary discussion of field evaporation in two-electrode system.⁴ Tsong also shows that field evaporation of alkali metals and Zn and Au as singly charged negative ions requires the lowest fields. In this paper we present a detailed calculation for field evaporation of Au in the double-electrode system. Our calculation shows that the favored ion species should be the doubly charged negative ions; the calculated field required for this ion species is also much closer to the observed value in the STM experiment.

We use the charge-exchange model⁵ for the present study. Two methods, an effective binding potential method (EBPM) developed by Gollisch⁶ and an embedded-atom method (EAM) developed by Daw and co-workers,⁷ are used to calculate the potential energy curves of the atom-surface interaction. In the former method, the effective binding potential takes the form

$$U_i = b \sum_{\substack{j=1 \\ j \neq i}}^N [Q_{ij}(r_{ij})]^{\mu S \lambda} - \left(a \sum_{\substack{j=1 \\ j \neq i}}^N [Q_{ij}(r_{ij})]^{\lambda} \right)^{\mu}. \quad (1)$$

For a homonuclear system Q_{ij} describes the binding between two atoms located at \mathbf{r}_i and \mathbf{r}_j ; b , a , and λ are potential parameters; S is the anharmonicity; and μ is a constant. Q_{ij} is identified to be the overlap integral between two atoms at \mathbf{r}_i and \mathbf{r}_j , or

$$Q_{ij}(r_{ij}) = \int \rho_i(\mathbf{r}) \rho_j(\mathbf{r}) d\mathbf{r}. \quad (2)$$

The spherically symmetric atomic charge densities $\rho_i(\mathbf{r})$ Gollisch⁶ used were obtained by solving the relativistic Kohn-Sham equations with the $X\alpha$ approximation for exchange and correlation. These results are fitted to the form for Q_{ij} given by two exponentials,

$$Q_{ij}(r_{ij}) = c_1 e^{-p_1 r_{ij}} + c_2 e^{-p_2 r_{ij}}, \quad (3)$$

where for Au, $c_1 = 59.2$, $c_2 = 452.00$, $p_1 = 1.44$ a.u.⁻¹, $p_2 = 2.04$ a.u.⁻¹, $b = 1.36157$ Ry, $a = 0.19369$ Ry^{5/3}, $\lambda = 0.69370$, $\mu = 0.60$, and $S = 2/\mu$. In Eq. (1), the first term represents the repulsive part.

In the embedded-atom method,⁷ the energy of an atom in question is a functional of the density of the unperturbed host. The total energy of the solid is expressed as

$$E_{\text{total}} = \sum_{i=1}^N F_i(\rho_{h,i}) + \frac{1}{2} \sum_{\substack{i,j=1 \\ i \neq j}}^N \phi_{ij}(r_{ij}) \quad (4)$$

where ϕ_{ij} is the short-range (doubly screened) pairwise interaction between the cores. If the host density is approximated by the sum of the atomic densities,

$$\rho_{h,i} = \sum_{\substack{j=1 \\ j \neq i}}^N \rho_j^q(r_{ij}), \quad (5)$$

then the energy is a simple function of the positions of the atoms. The pair repulsion term is assumed to have the form

$$\phi_{ij}(r) = z_i(r) z_j(r) / r, \quad (6)$$

where

$$z(r) = z_0(1 + \beta r^\nu)e^{-\alpha r}. \quad (7)$$

The functions $F_i(\rho)$ and ϕ_{ij} are determined empirically by fitting to the sublimation energy, equilibrium lattice constant, elastic constants, and vacancy formation energies of pure metals and the heats of solution of binary alloys.⁷ For Au the values are $z_0 = 11.0e$, $\alpha = 1.4475 \text{ \AA}^{-1}$, $\beta = 0.1269$, and $\nu = 2$. Daw and co-workers⁷ used Hartree-Fock wave functions and assumed that the density was given by

$$\rho^a(r) = n_s \rho_s(r) + n_d \rho_d(r), \quad (8)$$

where $n_s = 1.089$ and $n_d = 9.911$ for the s and d wave functions.

To provide consistency in the comparison between the potentials obtained from the two methods, the binding energy of a Au atom in a hollow site on the Au (100) surface is scaled to a value of 3.5 eV for both of these potentials, a value consistent with the cohesive energy of 3.93 eV for Au. For our calculations, the Hartree-Fock charge densities given by McLean and McLean⁸ for Au are used and scaled to yield a binding energy of 3.5 eV.

For the ionic potential of positive ions in an applied field F , we use

$$U_i^{n+} = \sum_{i=1}^n I_i - n\phi - neFz + U_i + U_{ic} \quad (9)$$

where n is the charge state, I_i is the ionization energy, ϕ is the work function, U_i is the image potential, and U_{ic} is the ion core repulsion term which is taken to be the first term of Eq. (1) for the EBPM and given by Eq. (6) for the EAM. For the single-electrode system of the FIM, the simple image potential term is used. For the double-electrode system of the STM, the classical multiple image interaction is approximated by⁹

$$U_i(z) = -\frac{(ne)^2}{d} \left[(\ln 2 - 1) + \left(\frac{z - \frac{1}{2}d}{d} \right)^2 + \frac{d^2}{d^2 - 4(z - \frac{1}{2}d)^2} \right]. \quad (10)$$

The electrodes are located at $z = 0$ and $z = d$. For the case of negative ion emission in an applied field F ,⁴

$$U_i^{n-} = n\phi - E_{\text{aff}}^{n-} + U_i - neFz + U_{ic} \quad (11)$$

where E_{aff}^{n-} is the electron affinity of the $n-$ ion. We use the same core repulsive term for the ions.

The potential energy curves of a Au atom interacting with a Au (100) surface derived from the two methods agree with each other fairly well. The EBPM gives a potential of slightly longer range [Fig. 1(a)]. Using parameters of Au atoms listed in Table I of Ref. 4 and the atomic and ionic potentials discussed above, one can now calculate the evaporation fields of ions of different charge states following the methods described in Ref. 4. In this work, we further reason that although Au^{2-} may not be stable in free space, during field evaporation it can "exist" in an applied field in the spatial region where the ionic curve is

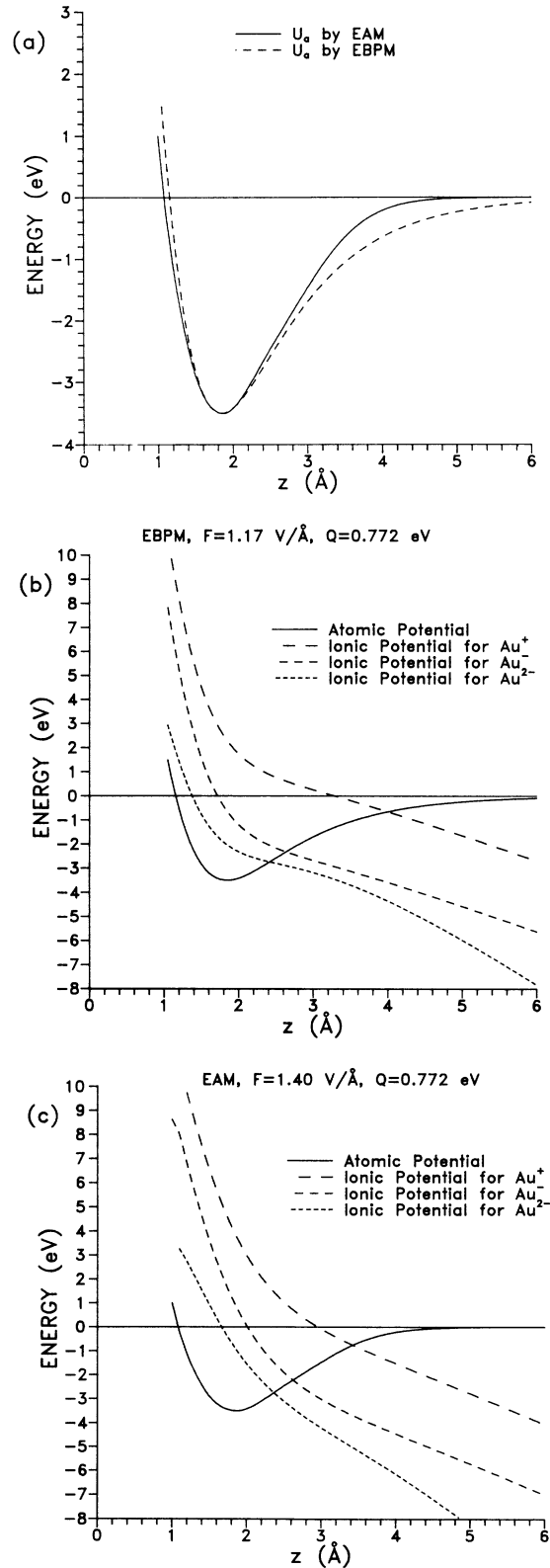


FIG. 1. (a) Atomic curves of a Au atom interacting with a Au (100) surface, obtained from the EBPM and EAM. (b) Atomic and ionic curves of Au, Au^+ , Au^{1-} , and Au^{2-} in an applied field of 1.17 V/\AA in a single-electrode system obtained from the EBPM. (c) Similar curves as in (b) at $F = 1.40 \text{ V/\AA}$ obtained from the EAM.

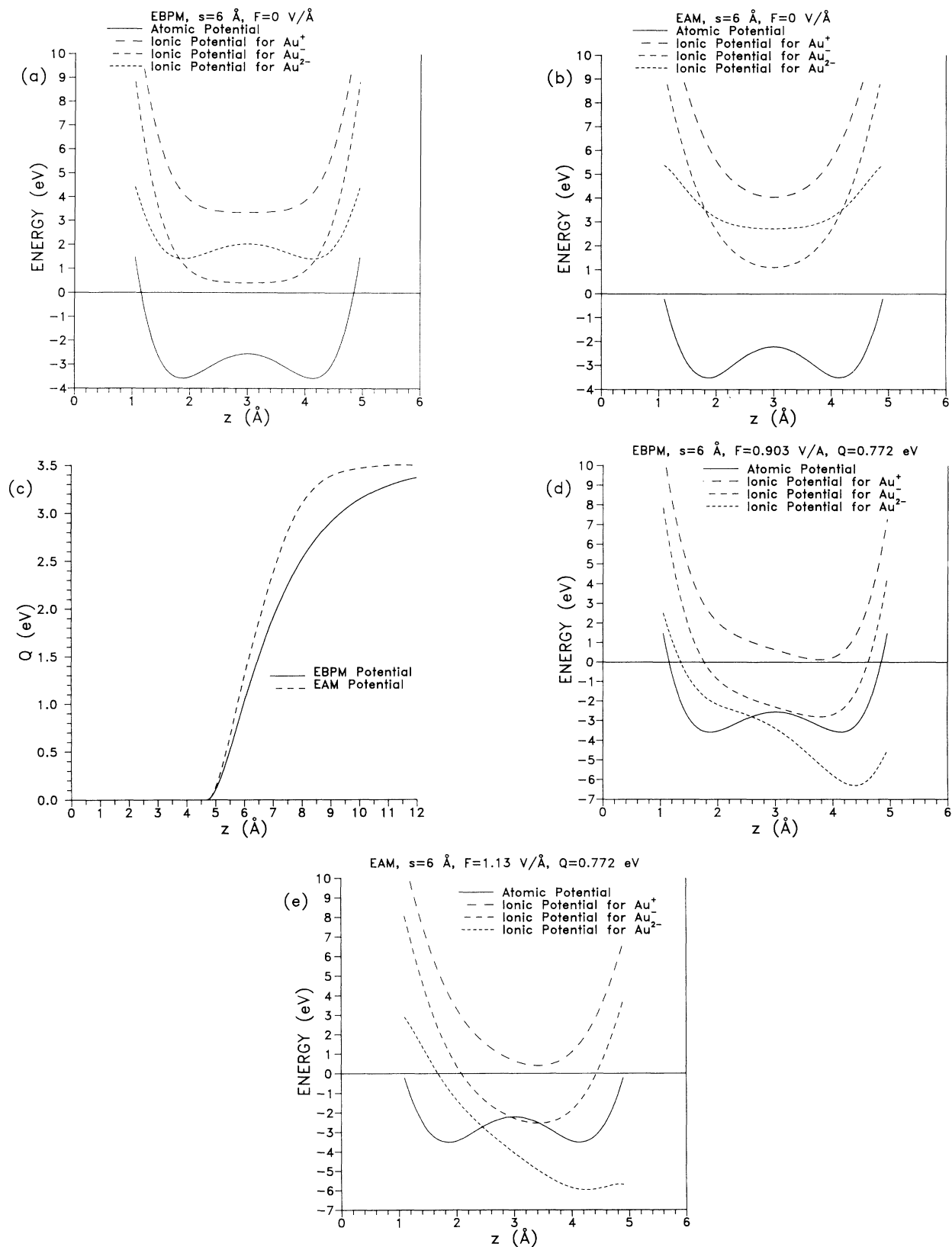


FIG. 2. (a) Atomic and ionic curves in zero applied field in a double-electrode system of separation 6 \AA , obtained from the EBPM. (b) Similar curves as in (a) obtained from the EAM. (c) The barrier height of the double well atomic potential plotted as a function of the electrode separation. (d) Atomic and ionic curves of Au, Au^+ , Au^{1-} , and Au^{2-} in an applied field of 0.903 V/\AA , obtained from the EBPM. At this field, Q for Au^{2-} is reduced to 0.772 eV . (e) Similar curves as in (d) for $F=1.13 \text{ V/\AA}$ obtained from the EAM.

lower than the atomic curve. The electron affinity of Au^- is 2.31 eV. However, we are not able to find a value for Au^{2-} . Because of a screening effect, the repulsive potential of the two electrons in a Au atom will not exceed $14.4/d \sim 4.5$ eV where d is the atomic diameter in angstroms. Thus E_{aff}^{2-} will not be smaller than $E_{\text{aff}}^- - 4.5$ eV, or ~ -2 eV. For studying the effect of E_{aff}^{2-} , we take two values of E_{aff}^{2-} , 0 and -2 eV. In the single-electrode system of the FIM, the fields needed for field evaporating Au at a rate of 1 s^{-1} at 300 K, or with an activation energy of $Q = 0.772$ eV, as Au^+ , Au^- , and Au^{2-} are found to be 3.2, 2.0, and 1.4 V/Å, respectively, when EAM potentials are used, and to be 2.7, 1.4, and 1.2 V/Å, respectively, when the EBPM potentials are used. When E_{aff}^{2-} is taken to be -2 eV, the evaporation field of Au^{2-} changes to 1.8 and 1.6 V/Å for the EAM and EBPM methods, respectively. This calculation shows that field evaporation of gold as Au^{2-} can occur at a field considerably lower than that for either Au^{1-} or Au^+ . But in the FIM, when the negative field exceeds about 0.6 V/Å, the field emission current will be large enough to melt the tip by resistive heating; thus even if Au^- and Au^{2-} can in principle be formed, it is difficult to observe; or only field evaporation of Au^+ can be observed. Figures 1(b) and 1(c) show the atomic and ionic curves for field evaporation of these ion species based on the EBPM and EAM.

In the double-electrode system of the STM, due to the overlap of the two atomic potentials interacting with the electrodes, a double well structure is formed as shown in Figs. 2(a) and 2(b). An atom can be thermally activated from one electrode to the other. The activation barrier height Q depends on the distance between the electrodes as shown in Fig. 2(c). At room temperature, a transfer

rate of 1 s^{-1} can be expected when Q becomes ~ 0.772 eV; this occurs when the electrode separation is ~ 5.5 Å. However, an atom can be transferred from the tip to the sample and from the sample to the tip at the same rate. For a unidirectional transfer of atoms field evaporation may be used. In a double-electrode system, as the applied field is gradually increased, atoms will start to transfer from one of the electrodes to the other when the field reaches that required for an ion species of the lowest evaporation field (in magnitude) to start field evaporating. In Figs. 2(d) and 2(e), ionic curves of Au^+ , Au^- , and Au^{2-} at a field which can reduce Q to 0.772 eV for the ion species requiring the lowest field are shown. This field is 0.903 V/Å from the EBPM and is 1.13 V/Å from the EAM, and the ion species is Au^{2-} . In comparison, the fields needed to reduce Q to 0.772 eV for field evaporating as Au^- and Au^+ are 1.73 and 2.93 V/Å for the EBPM and 1.25 and 2.38 V/Å for the EAM. The two methods agree with each other fairly well in the general trend. In this calculation, the electrode separation is taken to be 6 Å and E_{aff}^{2-} is taken to be zero. The ionic potential of Au^{2-} is the lowest among these three charge states and is lower than the atomic potential when $z > 2.6$ Å as can be seen from these figures. When the applied field is gradually raised in a two-electrode system, Au^{2-} ions will start to emit from the negative electrode at ~ 1.1 V/Å before other ion species can emit. When E_{aff}^{2-} is taken to be -2 eV, the evaporation field change to 1.55 and 1.30 V/Å for the two methods, but the conclusions are unchanged.

This research was supported by National Science Council of Republic of China under Grant No. NSC 81-0208-M-001-19.

*Permanent address: Physics Department, The Pennsylvania State University, University Park, PA 16802.

¹E. W. Müller and T. T. Tsong, *Field Ion Microscopy. Principles and Applications* (Elsevier, New York, 1969); T. T. Tsong, *Atom-Probe Field Ion Microscopy* (Cambridge Univ. Press, New York, 1990).

²H. J. Mamin, P. H. Guethner, and D. Rugar, *Phys. Rev. Lett.* **65**, 2418 (1990).

³J. A. Stroscio and D. M. Eigler, *Science* **254**, 1319 (1991).

⁴T. T. Tsong, *Phys. Rev.* **B 44**, 13703 (1991).

⁵R. Gomer and L. W. Swanson, *J. Chem. Phys.* **38**, 1613 (1963).

⁶H. Gollisch, *Surf. Sci.* **166**, 87 (1986); **175**, 249 (1986).

⁷M. S. Daw and M. I. Baskes, *Phys. Rev.* **B 29**, 6443 (1984); S. M. Foiles, M. I. Baskes, and M. S. Daw, *ibid.* **33**, 7983 (1986).

⁸A. D. McLean and R. S. McLean, *At. Data Nucl. Data Tables* **26**, 197 (1981).

⁹G. Binnig, N. Garcia, H. Rohrer, J. M. Soler, and F. Flores, *Phys. Rev.* **B 30**, 4816 (1984).